Oxidation of sulfur dioxide over supported vanadia catalysts: molecular structure – reactivity relationships and reaction kinetics

Joseph P. Dunn[a], Harvey G. Stenger Jr.[b], Israel E. Wachs[*,b]

[a]BOC Gases Technology, 100 Mountain Avenue, Murray Hill, NJ 07974, USA
[b]Zettlemoyer Center for Surface Studies, Department of Chemical Engineering, Lehigh University, Bethlehem, PA 18015, USA

Abstract

The oxidation of sulfur dioxide to sulfur trioxide over supported vanadium oxide catalysts occurs as both a primary and secondary reaction in many industrial processes, e.g., the manufacture of sulfuric acid, the selective catalytic reduction of NO_x with ammonia and the regeneration of petroleum refinery cracking catalysts. This paper discusses the fundamental information currently available concerning the molecular structure and sulfur dioxide oxidation reactivity of surface vanadia species on oxide supports. Comparison of the molecular structure and reactivity information provides new fundamental insights on the following topics related to the catalytic properties of surface vanadia species during the sulfur dioxide oxidation reaction:

1. role of terminal V=O, bridging V–O–V and bridging V–O-support bonds,
2. number of surface vanadia sites required to perform SO_2 oxidation,
3. influence of metal oxide additives,
4. generation and influence of the surface sulfate overlayer,
5. effect of surface acidity on the reaction turnover frequency,
6. competitive adsorption between SO_2 and SO_3 and
7. reaction kinetics.

© 1999 Elsevier Science B.V. All rights reserved.

Keywords: Oxidation; Sulfur dioxide; Vanadia catalyst; Sulfur trioxide

1. Introduction

Sulfur dioxide, SO_2, is formed from both the oxidation of sulfur contained in fossil fuels and industrial processes that treat and produce sulfur-containing compounds. The catalytic oxidation of sulfur dioxide appears in numerous industrial processes and has a significant environmental impact because of the asso-ciated sulfur oxide, SO_x, emissions. Approximately two-thirds of the 50 billion pounds of sulfur oxides released annually in the United States are emitted from coal fired power plants [1]. Industrial fuel combustion and industrial processes (primarily sulfuric acid manufacture, petroleum refining and smelting of non-ferrous metals) account for the remainder of the emissions.

Sulfuric acid is the largest volume chemical currently produced in the world, approximately 95 billion pounds per year [2], and is manufactured by the

---

*Corresponding author. Tel.: +1-610-758-4274; fax: +1-610-758-6555; e-mail: iew0@lehigh.edu

contact process, which involves the high temperature catalytic oxidation of sulfur dioxide to sulfur trioxide over a unique supported liquid phase catalyst (silica supported vanadium pyrosulfate with alkali promoters). Under reaction conditions, 450–610°C, the active vanadia component of the catalyst exists as a molten salt forming a very thin liquid layer on the surface of the silica support (only 100–1000 Å thick). Sulfur dioxide oxidation to sulfur trioxide proceeds on both the active sites located in the interior of the liquid film and on the boundary between the film and the surface of the silica support [3–5]. Thermodynamically controlled equilibrium limitations exist at the temperatures necessary for the catalyst to activate, $T > 420°C$, and the conversion of the sulfur dioxide feed is incomplete with the very small unreacted portion typically being directly emitted into the environment.

In contrast to the sulfuric acid contact process, the oxidation of SO_2 to SO_3 is undesirable during the selective catalytic reduction (SCR) of nitrogen oxides (NO_x) found in the flue gas of power plants. SCR removes NO_x in the flue gas by reacting the nitrogen oxides with ammonia and oxygen to form nitrogen and water at approximately 370°C over titania supported vanadia catalysts (e.g., $V_2O_5/WO_3–MoO_3/TiO_2$). Under typical SCR design and operating conditions, NO_x reduction efficiency is directly proportional to the $NH_3:NO_x$ ratio up to NO_x reduction levels of about 80%. Operating with too high of a $NH_3:NO_x$ ratio can lead to unreacted ammonia bypassing the reactor, ammonia slip, where it readily combines with SO_3 at temperatures below 250°C to form ammonium sulfates, which can block the catalyst's pores and foul downstream heat exchangers [6]. This problem is so serious that industrial specifications for SCR processes include upper limits for the outlet concentration of sulfur trioxide corresponding to approximately 1–2% sulfur dioxide conversion. Several studies have investigated the development of catalysts capable of simultaneously suppressing the oxidation of sulfur dioxide to sulfur trioxide while efficiently promoting the selective catalytic reduction of nitric oxide [7–11]. The advantages of such catalysts would be:

1. the ability to install more intrinsically active SCR catalysts (e.g., higher vanadia loadings) without the fear of simultaneously increasing SO_3 production and

2. savings in operating costs generated by lowering SCR temperatures, without the worry of ammonium sulfate production and deposition.

Two new NO_x/SO_x removal techniques, SNO_x (Haldor Topsoe) and $DeSONO_x$ (Degussa), combine SCR technology with sulfuric acid production [12,13]. Flue gas is heated to 380°C and nitrogen oxides are removed via conventional SCR technology. The products are further heated to 420°C and the SO_2 is oxidized to SO_3 over a sulfuric acid contact catalyst. The sulfur trioxide is then contacted with water producing concentrated sulfuric acid. Any unreacted ammonia from the SCR reactor is oxidized to NO_x over the second catalyst bed, consequently, avoiding the formation of ammonium sulfates.

Sulfur oxide emissions from fluid catalytic cracking (FCC) units account for a sizable fraction of annual SO_x emissions and are increasingly being targeted by the Environmental Protection Agency (EPA). The amount of SO_x emitted from a FCC unit regenerator is a function of the quantity of sulfur in the feed, coke yield and conversion [14]. Typically, 45–55% of feed sulfur is converted to hydrogen sulfide in the FCC reactor, 35–45% remains in the liquid products, and about 5–10% is deposited on the catalyst in the coke [14,15]. The sulfur in the coke is oxidized to SO_2 (90%) and SO_3 (10%) in the FCC regenerator. Traditional techniques of SO_x control such as flue gas scrubbing and feedstock hydrodesulfurization are effective, but are labor and cost intensive. The least costly alternative is the use of a SO_x-reduction catalyst as an additive to the FCC catalyst inventory. The catalyst must be able to:

1. oxidize SO_2 to SO_3 in the FCC regenerator,
2. chemisorb the SO_3 in the FCC regenerator, and then
3. release it as hydrogen sulfide in the reducing FCC reactor.

Supported vanadia catalysts, such as Amoco's $DeSO_x$ catalyst ($V_2O_5/CeO_2/Mg_2Al_2O_5$), have demonstrated high activity towards these reactions.

In addition, petroleum refining operations such as FCC and hydrodesulfurization (HDS) yield hydrogen sulfide as an undesired product. The hydrogen sulfide is typically concentrated and fed to a Claus plant to produce elemental sulfur. However, due to equilibrium

limitations only 97% of the sulfur is recovered in the Claus plant and the tail gas, therefore, needs to be treated before being released to the atmosphere. The mobil oil SO_x treatment (MOST) process involves combusting the Claus tailgas with air, converting all of the sulfur species to SO_2 and SO_3. The SO_x is sorbed onto a $V_2O_5/CeO_2/Mg_2Al_2O_5$ spinel where it is later regenerated to produce concentrated H_2S and SO_2, which is recycled to the Claus plant for further processing [16].

In spite of the industrial importance and environmental consequences of the above catalytic oxidation processes involving sulfur dioxide, few fundamental studies have been performed on the kinetics and mechanism of sulfur dioxide oxidation with the exception of the unique sulfuric acid contact catalyst [3–5]. However, the studies on commercial sulfuric acid catalysts are not applicable to the environmental oxidation reactions over conventional solid metal oxide catalysts since the contact catalyst contains the active vanadia/alkali/sulfate component as a molten salt on the silica support. Current research into the oxidation of SO_2 to SO_3 over conventional supported vanadia catalysts has focused on establishing the fundamental kinetics and molecular structure-reactivity relationships of the oxidation reaction [17,18]. It is hoped that the insights generated from these studies will assist in:

1. the design of SCR DeNO$_x$ catalysts with minimal SO_2 oxidation activity,
2. the development of catalysts for low temperature (200–300°C) oxidation of SO_2 to SO_3 during sulfuric acid manufacture and,
3. improvements in additives for the simultaneous oxidation/sorption of sulfur oxides in petroleum refinery operations.

This report will attempt to summarize the current fundamental understanding of the scientific concepts guiding the oxidation of SO_2 to SO_3 over supported vanadia catalysts by correlating pertinent molecular-level structural information with the observed reaction kinetics. In addition, it is hoped that the information contained herein will lay the foundation for future studies of SO_2 oxidation over pollution control catalysts. Although widely used in petroleum refinery operations, vanadia supported on magnesium aluminate spinels ($Mg_xAl_2O_{3+x}$) will not be highlighted in this report due to the limited information available in the literature concerning the surface arrangement of these catalysts.

2. Synthesis of supported vanadia catalysts

Many different synthesis methods have been used in the preparation of supported vanadia catalysts: vapor phase grafting with $VOCl_3$ [19–21], non-aqueous impregnation with vanadium alkoxides [22,23] and vanadium acetate [24], aqueous impregnation of vanadium oxalate [25], as well as dry impregnation with crystalline V_2O_5 [26–29]. However, all the catalysts were found to contain the same surface vanadia species independent of the initial synthesis method after prolonged calcination [30]. The absence of a ''preparation memory effect'' is due to the high mobility of V_2O_5 (Tamman temperature of 370°C) and the strong driving force of the mixed oxide system to lower its surface free energy by forming a monolayer of surface vanadia species on the high surface free energy oxide support [26–29]. The formation of a monolayer is even observed during hydrocarbon oxidation reactions over physical mixtures of V_2O_5 and TiO_2 [31]. Thus, the same thermodynamically stable surface metal oxide species are formed independent of the specific synthesis method. In the case of silica supported vanadia catalysts, where different preparation methods can affect the surface coverage of the surface vanadia species, the same isolated surface vanadia species results from all the different syntheses. Commercial preparations usually employ aqueous impregnation with vanadium oxalate because of its high solubility in water and the absence of undesirable volatile organic solvents [32–36].

3. Characterization of supported vanadia catalysts

Surface vanadium oxide phases are formed when vanadium oxide is deposited on an oxide support (e.g., SiO_2, Al_2O_3, TiO_2, ZrO_2, CeO_2 and MgO) [37,38]. The supported vanadium oxide phase, like other supported metal oxide phases, can simultaneously exist in several different structural states (bulk crystallites, mixed phases with the support, or two-dimensional

overlayers). Recent developments in molecular characterization techniques have successfully demonstrated the capability to discriminate between the multiple vanadium oxide structures present in supported vanadia catalysts and provide information required to develop a molecular level understanding of these complex catalytic materials.

Several studies have shown that Raman spectroscopy can readily discriminate between different vanadium oxide structures with different coordinations and bond lengths [32,39,40]. Raman spectroscopy is an optical technique and, therefore, can be applied to study the structural changes of the surface vanadia species under in situ conditions where the environment around the catalyst is controlled (temperature, pressure and gas composition). The theory and application of Raman spectroscopy to catalytic material can be found elsewhere [41,42].

Infrared spectroscopy can also discriminate between various vanadium oxide structures. However, many of the oxide supports obscure the vibrations arising from the supported vanadium oxide phase because they absorb the infrared signal (especially below $1000 \, \text{cm}^{-1}$). For some systems it is at least possible to obtain the highest frequency of the surface vanadia species, which usually corresponds to the vanadium–oxygen terminal bonds [42–44]. Similar to Raman spectroscopy, infrared spectroscopy can be applied to study the structural changes of the surface vanadia species under in situ conditions. Adsorption of basic molecules (e.g., ammonia and pyridine) provides information about the distribution of surface Lewis and Bronsted acid sites [45,46]. IR also provides direct information about the interaction of vanadia species with the surface hydroxyls of oxide supports. Additional information about the theory and application of infrared spectroscopy to catalytic material can be found elsewhere [47].

The ^{51}V nucleus possesses excellent characteristics for NMR experiments due to its natural abundance (99.78%). These advantageous characteristics have resulted in a number of recent studies using solid state ^{51}V nuclear magnetic resonance (NMR) spectroscopy for the characterization of supported vanadium oxide catalysts [32,34,35,48]. The limitation of solid state ^{51}V NMR is that vanadium in the 4+ oxidation state broadens the NMR signal, and consequently, the signal due to the V^{5+} nucleus can be lost. Information about the theory and application of solid state ^{51}V NMR to supported vanadium oxide catalysts can be found elsewhere [47].

X-ray absorption spectroscopy takes advantage of intense synchrotron X-ray sources to determine the oxidation state and chemical environment around a specific element in the sample. X-ray absorption techniques (EXAFS/XANES) have been used to determine the molecular structures of the supported vanadium oxide phase with some success [49–51]. Furthermore, X-ray absorption spectroscopy can be used under in situ conditions. The disadvantage of the X-ray absorption techniques is that only an average signal of the different vanadium oxide structures is observed and hence, only the average structure can be obtained.

X-ray photoelectron spectroscopy (XPS) provides information on the oxidation state and dispersion in the surface region (2 to 20 atomic layers) of the catalyst [47]. However, molecular structural information of the surface vanadium oxide phase cannot be obtained using XPS since it cannot discriminate between different vanadium oxide structures possessing the same oxidation state. Furthermore, XPS requires high vacuum conditions for its operation and cannot be used under in situ conditions, but is especially useful when reduced vanadium oxide states are present.

Electron paramagnetic resonance (EPR) is also a bulk characterization technique that is effective in determining the nature of paramagnetic species, such as vanadium in the 4+ oxidation state, immersed in diamagnetic matrices [52]. This is possible since the g factor and hyperfine splitting, arising from an interaction of the unpaired electron with the ^{51}V nucleus, are extremely sensitive to the chemical environment around the paramagnetic V^{4+} ion. However, EPR studies are usually not amenable to in situ studies under reaction environments due to signal broadening at elevated temperatures [53]. An additional limitation of the EPR technique is that it is ideally applicable for isolated V^{4+} ions due to problems associated with signal broadening and spin–spin coupling for paired V^{4+} ions. In spite of the above potential complications, EPR is one of the few characterization techniques that can provide molecular structural information about reduced vanadium (IV) oxide species [54–59].

Ultra violet and visible (UV-vis) spectroscopy takes advantage of the different electronic transitions of metal ions that depend on the symmetry of the environment. The application of UV-vis spectroscopy for the study of supported vanadium oxide catalysts has also received some attention [60–62]. However, the origin of the specific electronic transition is sometimes difficult to isolate since the electronic transition depends on various parameters: local symmetry, overall symmetry, condensation degree, polarization effect and size of the counter cation and dispersion on a support [63]. The broad UV-vis bands can also decrease the sensitivity for certain species. However, UV-vis spectroscopy can be successfully applied to supported vanadium oxide catalysts when used in conjunction with other characterization techniques (e.g., Raman and NMR).

In, summary, the physical characterization techniques (e.g., Raman, NMR and IR) are essentially bulk techniques that take advantage of the surface nature of the supported vanadium oxide phase. Of these techniques, Raman and solid state ^{51}V NMR spectroscopy are best suited for molecular characterization of vanadium (V) oxide. X-ray absorption (EXAFS/XANES) and IR spectroscopies are good complimentary techniques when used in conjunction with Raman and NMR. XPS can be used only to study the oxidation state and dispersion of the supported vanadium oxide phase. EPR and X-ray absorption spectroscopy can provide structural information about reduced V^{4+} species. UV-vis, however, is not a very informative characterization technique for supported vanadia catalysts when applied independently. Characterization techniques most suitable for in situ reaction studies are Raman, IR, X-ray absorption (EXAFS/XANES), and to a limited extent ^{51}V NMR, EPR and UV-vis.

4. Molecular structures of supported vanadia catalysts

To fully understand the molecular structure-reactivity relationships for the oxidation of sulfur dioxide over supported vanadia catalysts, a detailed knowledge of the molecular structures of the vanadia surface species is required. The wide array of spectroscopies mentioned above have been applied to the characterization of the supported vanadia catalysts. These studies have revealed that the surface structures and oxidation states of the surface vanadia species on various supports (e.g., SiO$_2$, Al$_2$O$_3$, TiO$_2$, ZrO$_2$, CeO$_2$ and MgO) are dynamic and strongly dependent on the particular environment (oxidizing and reducing atmospheres, moisture and temperature). Unfortunately, the dynamic nature of the surface vanadia species has resulted in some confusion in the published literature since many studies have compared measurements taken under different experimental conditions. In order to minimize such problems, the present paper will only focus on experimental results obtained under well defined conditions with monolayer and sub-monolayer loaded vanadia catalysts.

4.1. Dehydrated conditions

Dehydrated conditions are created by heating the catalyst to elevated temperatures, from 300°C to 700°C, in a flowing oxygen-containing stream for at least 30 min. Such treatment desorbs adsorbed moisture from the catalyst surface and maintains the surface vanadia species in the fully oxidized V^{5+} oxidation state [35].

4.1.1. Acid/base properties of supported vanadia catalysts

Most support oxides of interest in catalysis (e.g., SiO$_2$, Al$_2$O$_3$, TiO$_2$, ZrO$_2$, CeO$_2$ and MgO) contain a variety of surface sites including surface hydroxyl groups and coordinatively unsaturated Lewis acid/base sites [64]. The site mixture depends on the nature of the oxide, but it can also vary according to the preparative method used, conditions of activation and on the presence of foreign impurities. Upon addition, vanadia species titrate the surface hydroxyls and become anchored to the supporting oxide through bridging vanadium–oxygen–support cation bonds. The surface vanadia species possess both Lewis and Bronsted acid properties and the ratio of Bronsted acidity to Lewis acidity increases with surface vanadia coverage [65,66]. The basicity of the surface vanadia species is negligible [67–69].

4.1.2. V$_2$O$_5$/SiO$_2$ catalysts

There is a unanimous agreement among all researchers that the dehydrated surface vanadia species on silica consist of isolated VO$_4$ units consisting
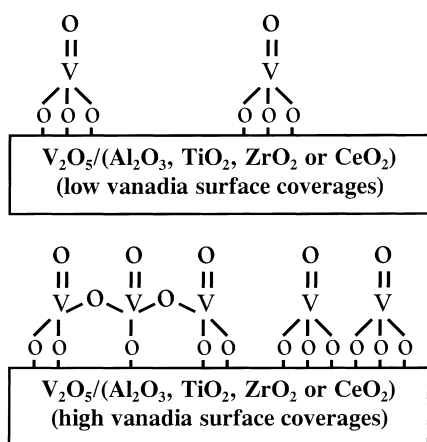
Fig. 1. Proposed structure of vanadium oxide species on Al_2O_3, TiO_2, ZrO_2 and CeO_2 supports under dehydrated conditions.

of one terminal V=O bond and three bridging V–O–Si bonds (trigonal pyramidal configuration). The maximum surface coverage achieved to date on silica without formation of microcrystalline V_2O_5 particles, ~4 V atoms/nm^2, corresponds to that expected for a monolayer of isolated surface VO_4 units [70].

4.1.3. $V_2O_5/(CeO_2, ZrO_2, TiO_2$ and $Al_2O_3)$ catalysts

The dehydrated surface vanadia species on other oxide supports (ceria, zirconia, titania and alumina) possess essentially identical molecular structures [37,38,43,44,71–73]. The dehydrated surface vanadia species on these oxide supports are primarily present as both isolated (low coverages) and polymerized (high coverages) VO_4 units with similar ratios of the species at any given vanadium oxide surface coverage. As shown in Fig. 1, the molecular structures of the surface vanadia species are tentatively thought to consist of a terminal V=O and three bridging vanadium–oxygen–support (V–O–M) bonds for the isolated species, and a terminal V=O bond with one or two bridging V–O–M and one or two bridging V–O–V bonds for the polymerized species. There may also be a trace of surface VO_6 units (octahedral coordination) present at monolayer coverages, but additional studies are required to establish this possibility. At coverages exceeding a monolayer (approximately 13 μmol V^{5+}/m^2 or 8 V atoms/nm^2 for CeO_2, ZrO_2, TiO_2 and Al_2O_3), microcrystalline V_2O_5 particles are formed as a separate three-dimensional phase on

the two-dimensional surface vanadia overlayer (i.e., the isolated and polymerized surface vanadia species).

4.1.4. V_2O_5/MgO catalysts

Unlike the above supported vanadia catalysts, the magnesia supported vanadia catalyst system cannot form a complete close-packed surface vanadia monolayer because of the strong acid–base reaction between acidic vanadia and basic magnesia. The interaction between vanadia and magnesia results in the formation of a mixed metal oxide rather than a stable surface vanadia overlayer on the magnesia support [72–74]. The vanadia coordination in bulk V–Mg–O mixed metal oxide catalysts consists of VO_4, VO_5 and VO_6 units. Thus, the magnesia supported vanadia catalyst system possesses both surface and bulk vanadia species.

4.1.5. Influence of metal oxide additives on supported vanadia catalysts

Metal oxide additives present in multicomponent vanadia catalysts can be classified into two broad categories:

1. non-interacting additives, which preferentially coordinate with the oxide support rather than the surface vanadia species under dehydrated conditions and
2. interacting additives, which preferentially coordinate with the surface vanadia species rather than the oxide support under dehydrated conditions.

Typical non-interacting additives are surface oxides of Co, Fe, Mo, Nb, Ni, S and W [75–79]. Non-interacting additives can only indirectly affect the molecular structure of the vanadia species via lateral interactions. Such lateral interactions have been found to increase the ratio of polymerized to isolated surface vanadia species in supported metal oxide catalysts: Fe>Ni–Co>S>Mo–W>Nb.

Typical interacting additives are oxides of P and Zn and alkali/alkaline earth oxides (Ca, Na, K, etc.) that tend to complex with the acidic surface vanadia species [78,79]. The basic alkali/alkaline earth additives do not change the trigonal–pyramidal configuration of the dehydrated surface vanadia species on most supports, but do affect the V–O bond lengths by significantly increasing the V–O bond length and, consequently, decreasing the bridging V–O bond

lengths [72,73,78,79]. Thus, the basic surface additives do not form three-dimensional mixed vanadate compounds, but just alter the V–O bond lengths of the surface vanadia species. However, the interaction between P and surface vanadia species can result in the formation of crystalline $VOPO_4$ phases, at the expense of the surface vanadia phase, after calcination due to the strong interaction between the two oxides [78,80,81]. The formation of crystalline $VOPO_4$ phases can only be avoided if the surface phosphorous oxide species is first anchored to the oxide support surface via calcination before the introduction of the vanadia precursor [80,81]. Thus, interacting additives can both modify the local structure of the surface vanadia species, affecting the V–O bond lengths, as well as form crystalline mixed metal oxide phases because of their chemical affinity for vanadia.

4.2. Water vapor containing environments

The influence of water vapor/oxygen environments at elevated temperatures, 120–500°C, upon the dehydrated surface vanadia species has recently been investigated due to the high levels of moisture (2–10 vol%) present in many air pollution control applications [82]. For the silica supported vanadia catalysts, moisture has no effect on structure of the surface vanadia species, revealing silica's hydrophobic nature. For the other supported vanadia catalysts (V_2O_5 on CeO_2, ZrO_2, TiO_2 and Al_2O_3), the presence of water vapor does have an effect on the surface vanadia species. Above 300°C, the surface vanadia species retain their structures despite small amounts of adsorbed moisture present on the catalyst surface. Isotopic oxygen-18 exchange experiments reveal that the reversibly adsorbed moisture is able to rapidly undergo oxygen exchange with the terminal V=O bond of the surface vanadia species at these high temperatures. At approximately 200°C and below, monolayer quantities of adsorbed moisture are present on the supported vanadia catalysts, extensively solvating the surface vanadia species (and any other surface metal oxide species).

4.3. Sulfur oxide containing environments

The adsorption and oxidative adsorption of sulfur dioxide onto the various metal oxide supports have been extensively investigated in recent years with numerous spectroscopic (e.g., IR [83–89], Raman [90–93] and XPS [92,94–96]) and thermal (e.g., TGA [83,86,87,89,91], TPD [83,91,97] and DTA [67–69]) techniques. MgO, CeO_2 and Al_2O_3 have received much attention due to their ability to act as SO_x transfer catalysts [98–101]. Sulfated TiO_2 and ZrO_2 are representatives of a class of metal oxides known as solid-superacids, which are highly reactive for the isomerization of hydrocarbons and dehydration of alcohols [102]. In contrast, fewer studies have focused on adsorption of SO_2/SO_3 on supported vanadia catalysts [67–69,93,103]. Supported vanadia catalysts, e.g., V_2O_5/WO_3–MoO_3/TiO_2, are used extensively in the selective catalytic reduction of NO with NH_3 where they are exposed to moderate levels of SO_x (∼500 ppm of SO_x) [6]. Bronsted acid sites, which promote the adsorption of ammonia during the SCR reaction, are created from the interaction of adsorbed sulfate species and water [104,105].

4.3.1. Unpromoted metal oxide supports

Upon exposure to SO_2, in the absence of gas phase oxygen, either physisorbed sulfur dioxide (SO_{2-}) or chemisorbed sulfite (SO_{3-}) surface species are formed on metal oxide surfaces, depending on the adsorption temperature and the specific metal oxide support [83,106]. The mildly acidic sulfur dioxide acts as an electron acceptor and adsorbs on basic surface sites, but fails to interact with neutral and acidic surface sites. Since only a fraction of the support hydroxyls meet the criteria necessary for SO_2 adsorption, maximum surface coverages of SO_{2-} and SO_{3-} species correspond to less than a theoretical monolayer (∼4 S atoms/nm^2 for isolated species) [71]. This selective titration allows the concentration of chemisorbed sulfite species to be used as a measure of the relative basicity of the supports: MgO–$CeO_2 \gg ZrO_2 > TiO_2$–$Al_2O_3 \gg SiO_2$ [70].

Sulfates (SO_4^-) are produced when surface sulfite (SO_3^-) species titrate adjacent sites and form additional bonds to the metal oxide support. The transformation of surface sulfite species into the more thermodynamically stable sulfate species will proceed on all supports upon exposure to gas phase oxygen at temperatures above 200°C [83,106]. The creation of a surface sulfate overlayer may also occur at temperatures above 200°C during the adsorption of sulfur

trioxide, oxidative adsorption of sulfur dioxide and hydrogen sulfide [86,94,95,107].

4.3.1.1. Sulfated SiO₂. SiO$_2$ does not contain basic surface hydroxyl functionalities and, therefore, does not form stable surface sulfate overlayers in the presence of sulfur oxides and excess oxygen at elevated temperatures [84].

4.3.1.2. Sulfated Al₂O₃, TiO₂ and ZrO₂. Oxide supports such as Al$_2$O$_3$, TiO$_2$ and ZrO$_2$ contain basic surface hydroxyls and can form stable sulfate overlayers by heating in the presence of either sulfur trioxide, sulfur dioxide or hydrogen sulfide and excess oxygen. Tridentate SO$_4$ surface species, i.e., (Ti–O)$_3$S=O and (Al–O)$_3$S=O, have been observed on sulfated TiO$_2$ and Al$_2$O$_3$ under dehydrated conditions [85]. In addition, two tridentate SO$_4$ species and a polymeric S$_2$O$_7$ species were shown to exist on sulfated ZrO$_2$ [64].

Upon exposure to water vapor, at temperatures between 200°C and 400°C, the tridentate sulfates present on alumina, titania and zirconia supports are converted into protonated bidentate surface species [85]. This lowers the stability of the surface sulfate species and increases the Bronsted acidity of the support via the production of moderately acidic S–O–H surface functionalities [104,105].

4.3.1.3. Sulfated CeO₂ and MgO. On the oxide supports possessing the most basic surface hydroxyls (CeO$_2$ and MgO), sulfate groups form easily upon exposure to sulfur trioxide or either sulfur dioxide or hydrogen sulfide and excess oxygen. Strong interactions between the adsorbed sulfate groups and the supporting oxide lead to a wide range of surface sulfate and bulk sulfur–oxy–support species being formed. Sulfation of the highly basic CeO$_2$ support produces both surface and bulk-like sulfate species [87,90]. The former is thought to have a tridentate SO$_4$ structure, i.e., (Ce–O)$_3$S=O, while bulk-like species have been shown to have a more ionic character [87]. In the absence of gas phase oxygen, strong interactions between the CeO$_2$ support and chemisorbed sulfur dioxide promote the oxidation of sulfite species to both surface and bulk-like sulfates with an accompanying reduction of CeO$_2$ into Ce$_2$O$_3$ [87].
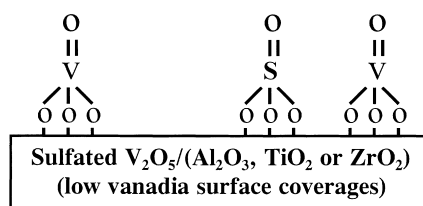

Fig. 2. Proposed structure of sulfated supported vanadium oxide catalysts under dehydrated conditions (vanadia surface coverage <0.3 monolayers).

Two kinds of sulfate species were shown to form on MgO depending on the sample surface area and the amount of SO$_2$ introduced. On a low surface area sample (∼10 m^2/g), bulk-like sulfate was the major product, whereas, both surface and bulk-like sulfates were formed on a high surface area sample (∼290 m^2/g). Oxygen-18 exchange experiments indicated that the surface sulfate has a bidentate configuration with a trigonal O=S=O terminal group, i.e., (Mg–O)$_2$(S=O)$_2$ [108].

4.3.2. Supported vanadia catalysts (sub-monolayer vanadia coverages)

As shown in Fig. 2, the surface sulfate species present on sub-monolayer supported vanadia catalysts preferentially coordinate with the oxide supports rather than the surface vanadia species under dehydrated conditions and, consequently, can only indirectly affect the molecular structures of the supported vanadia species via lateral interactions [93]. In addition, the amount of adsorbed sulfate appears to decrease more rapidly than one may expect from simple geometrical coverage by surface vanadate species [67–69,93]. Similar coverage effects have been made for sulfated MoO$_3$/Al$_2$O$_3$ catalysts and can be explained by the observation that while surface sulfate species titrate only the most basic hydroxyls (IR bands at 3785, 3740 and 3705 cm^{-1}), surface molybdate species titrate both basic and neutral hydroxyls (IR bands at 3785, 3740, 3705 and 3590 cm^{-1}) forming a complete monolayer [92]. At low MoO$_3$ and V$_2$O$_5$ loadings, the molybdena and vanadia surface species preferentially titrate the basic hydroxyls, consuming the sites capable of sulfur dioxide adsorption. The increased Bronsted acidity exhibited by the sulfated zirconia, titania and alumina supports in the

presence of water vapor is also found for sulfated supported vanadia catalysts [109–112].

4.3.3. Supported vanadia catalysts (monolayer vanadia coverage)

Vanadium oxide–sulfur oxide surface complexes must be formed during the sulfur dioxide oxidation reaction. The difficulties in detecting the sulfation of surface vanadia species have been demonstrated in several recent studies. Following oxidative adsorption of sulfur dioxide at $175^{\circ}C$ on a monolayer V_2O_5/TiO_2 ($\sim 13\,\mu$mols V^{5+}/m^2) catalyst the uptake of sulfur dioxide was undetectable ($<0.05\,\mu$mols SO_2/m^2) [103]. Similarly, sulfur dioxide has been employed as a probe for basic sites present on V_2O_5/Al_2O_3 catalysts at $80^{\circ}C$. As vanadia surface coverage approached a monolayer ($\sim 13\,\mu$mols V^{5+}/m^2), the volumetric uptake of sulfur dioxide fell below the limit of detection ($<0.09\,\mu$mols SO_2/m^2) of the adsorption chamber used in the study [67–69]. The same study failed to detect the adsorption of sulfur dioxide onto bulk V_2O_5 and monolayer V_2O_5/SiO_2 catalysts.

Unfortunately, no in situ spectroscopic studies attempting to identify vanadium oxide–sulfur oxide reaction intermediates have been performed. However, it is doubtful that presently available spectroscopic techniques could detect the extremely small concentration of surface complexes believed to exist under reaction conditions, since the quantity of basic sites capable of adsorbing sulfur dioxide on monolayer supported vanadia catalysts is negligible. In addition, Raman and IR spectroscopy studies of dehydrated sulfate promoted monolayer supported vanadia catalysts fail to detect spectral bands characteristic of vanadium oxide–sulfur oxide surface complexes [93]. The interaction of sulfur trioxide and monolayer V_2O_5/CeO_2 at elevated temperatures has been shown to disturb the surface VO_4 tetrahedra and results in the generation of bulk cerium vanadate and cerium sulfate [93].

4.4. Reducing environments

Exposure of the surface V^{5+} species to reducing H_2, H_2S and CO environments results in the formation of surface V^{4+} and V^{3+} species [54–59,113–118]. The oxide supports (ZrO_2, TiO_2, Al_2O_3 and SiO_2) are not reduced during the reduction of the surface vanadia species with the exception of CeO_2, which exhibits the presence of minor amounts of reduced Ce_2O_3 [119,120]. The average oxidation states of the reduced surface vanadia species have been determined by temperature programmed reduction (TPR) and thermogravimetric measurements (primarily for alumina and silica catalysts) [113,114]. More specific information about the distribution of oxidation states has been obtained with XPS studies [115–118]. However, there currently appears to be a lack of consensus among these publications as to the distribution of V^{4+} and V^{3+} species. In addition, there also does not appear to be any consensus about the structural assignments of the V^{4+} species in supported vanadia catalysts: distorted VO_6, square–pyramidal VO_5 or trigonal–pyramidal VO_4 V^{4+} species [54–59]. Thus, dependable studies addressing the molecular structures of the reduced surface vanadia species are rare at present and a more systematic series of experiments are required to determine the influence of various variables (specific oxide support, specific reducing gas, steam, temperature, etc.).

5. SO_2 oxidation reactivity of surface vanadia species

5.1. Molecular structure–reactivity relationships

The catalytic properties of several well-defined model supported vanadia catalysts have recently been probed with the oxidation of sulfur dioxide to sulfur trioxide [17,121]. The reactivity properties of these catalysts are compared with the corresponding structural information presented above in order to develop molecular structure–reactivity relationships for supported vanadia catalysts during the sulfur dioxide oxidation reaction.

5.1.1. Role of bridging V–O–V bonds

Several recent in situ Raman studies have demonstrated that the ratio of bridging V–O–V bonds to terminal V=O bonds increases with surface vanadia coverage on oxide supports, with the exception of V_2O_5/SiO_2 which only possesses isolated surface vanadia species and no bridging V–O–V bonds [37,38]. Consequently, the role of V–O–V bridging

bonds in oxidation reactions can be chemically probed by examining the reaction turnover frequency, TOF – the number of SO_2 molecules oxidized per surface vanadia site per second, as a function of surface vanadia coverage. The sulfur dioxide oxidation activity of V_2O_5/TiO_2 catalysts of variable loading (1–6% V_2O_5, corresponding to 0.16–1.0 theoretical monolayers ($\sim$1.5–8 V atoms/nm^2) for a 50 m^2/g Degussa P-25 TiO_2 support) was determined between 200°C and 400°C [17]. The magnitude of the turnover frequency for 1% V_2O_5/TiO_2 varied from 3×10^{-6} s^{-1} at 200°C to 1×10^{-4} s^{-1} at 400°C. The results showed that the turnover frequency is approximately constant as the surface vanadia loading is varied up to monolayer coverage. Therefore, the reactivity of titania supported vanadia catalysts for the oxidation of sulfur dioxide to sulfur trioxide is independent of the surface density of bridging V–O–V bonds, which indicates that these bonds do not play a critical role in the overall SO_2 oxidation kinetics. In addition, a reaction requires two or more surface vanadia sites to proceed would exhibit higher turnover frequencies at higher surface coverages due to the increasing number of polymerized surface vanadia species present at higher surface coverages. Thus, the observation that the SO_2 oxidation turnover frequency does not increase with increasing surface coverage by surface vanadia species indicates that only one surface vanadia site is necessary for the SO_2 oxidation to proceed. In summary, the bridging V–O–V bonds do not play a critical role in SO_2 oxidation kinetics and only one surface vanadia site appears to be required for this reaction. Similar trends in TOF versus surface vanadia coverages were shown to exist for ceria, zirconia, alumina and silica supported vanadia catalysts.

5.1.2. Role of the terminal V=O bond

The terminal V=O bonds can also be directly monitored with in situ Raman spectroscopy during oxidation reactions. The vibrational frequency of the terminal V=O is directly related to its bond strength (stronger or shorter bonds vibrate at higher cm^{-1} and weaker or longer bonds vibrate at lower cm^{-1}) [37,38]. Sulfur dioxide oxidation experiments over several well characterized supported vanadia catalysts ($V_2O_5/(Al_2O_3, TiO_2, ZrO_2$ or CeO_2)) revealed that while the catalysts possessed essentially the same terminal V=O bond strength (1025–1031 cm^{-1}), the

SO_2 oxidation TOFs varied by more than an order of magnitude: V_2O_5/CeO_2>V_2O_5/ZrO_2, V_2O_5/TiO_2>V_2O_5/Al_2O_3 [17]. Consequently, the SO_2 oxidation TOFs do not correlate with the characteristics of the terminal V=O bond and suggests that this bond does not play a critical role in this oxidation reaction. A similar lack of correlation between the terminal V=O bond characteristics and propane, butane and methanol oxidation TOFs was also previously found [122–124].

5.1.3. Role of bridging V–O–support bonds

The sulfur dioxide oxidation reactivity is apparently related to the bridging V–O–M bond since changing the specific oxide support ligand alters the turnover frequency by more than an order of magnitude [17]. The only significant differences between the surface vanadia species on the various oxide supports are the oxide support ligands (e.g., Ce, Zr, Ti, or Al). The electronegativity of the oxide support cation affects the electron density on the bridging V–O–M oxygen: a lower cation electronegativity will result in a slightly higher electron density (more basic V–O–M oxygen) and a higher cation electronegativity will result in a slightly lower electron density (less basic V–O–M oxygen). An inverse correlation between the Sanderson electronegativities [125] of the oxide support cations and the sulfur dioxide oxidation turnover frequencies appears to exist; the lower the oxide support cation electronegativity the higher the sulfur dioxide oxidation turnover frequency [17]. Therefore, the more basic the bridging V–O–M bond the higher the activity towards SO_2 adsorption and subsequent oxidation of the acidic sulfur dioxide molecule. Conversely, a less basic bridging oxygen depresses the adsorption of sulfur dioxide and its oxidation. Thus, it appears that the catalysts exhibiting higher turnover frequencies contain a higher percentage of surface vanadia sites adsorbing sulfur dioxide and, subsequently, undergoing redox cycles under reaction conditions.

The above analysis may also be applied to other catalytic oxidation reactions over supported vanadia catalysts. The mechanism and kinetics of methanol oxidation to formaldehyde over vanadia catalysts have been extensively examined in recent years [126]. It has been proposed that methanol adsorbs at a bridging vanadium–oxygen–support (V–O–M) bond via proto-

nation of the bridging oxygen (H–O–M) and formation of a methoxy (V–OCH$_3$) intermediate. The rate determining step is the subsequent breaking of a methyl C–H bond to form formaldehyde. The trend in turnover frequencies for oxidation of the mildly acidic methanol molecule (V/Ce>V/Zr, V/Ti>V/Nb>V/Al≫V/Si) follows the same pattern as that observed for sulfur dioxide oxidation and inversely correlates with the Sanderson electronegativities of the support cations.

5.1.4. Influence of metal oxide additives

The effect of various metal oxide additives on the SO$_2$ oxidation activity of supported vanadia catalysts depends on the nature of the additive. The negative effect of interacting additives, such as GeO$_2$ and ZnO, on SO$_2$ oxidation TOFs over V$_2$O$_5$/TiO$_2$ catalysts has been reported in the literature [7] and is most likely due to vanadia–additive compound formation. Potassium oxide has been shown to substantially retard the SO$_2$ oxidation activity of V$_2$O$_5$/TiO$_2$ catalysts through direct interaction of the K$_2$O with the surface vanadia species and the reduction of its redox potential [127].

Non-interacting additives provide additional surface sites upon which the oxidation of SO$_2$ to SO$_3$ can proceed and, therefore, increase the catalytic activity of the promoted catalyst. This effect only lasts as long as the total surface coverage of (vanadia+additive) is less than a monolayer and the redox activity of the additive is greater than that of the supporting oxide it covers.

Dunn et al. [127] measured the SO$_2$ oxidation activity of several well characterized binary (e.g., V$_2$O$_5$/TiO$_2$, Fe$_2$O$_3$/TiO$_2$, Re$_2$O$_7$/TiO$_2$, CrO$_3$/TiO$_2$, Nb$_2$O$_5$/TiO$_2$, MoO$_3$/TiO$_2$ and WO$_3$/TiO$_2$) and ternary (e.g., V$_2$O$_5$/Fe$_2$O$_3$/TiO$_2$, V$_2$O$_5$/Re$_2$O$_7$/TiO$_2$, V$_2$O$_5$/CrO$_3$/TiO$_2$, V$_2$O$_5$/Nb$_2$O$_5$/TiO$_2$, V$_2$O$_5$/MoO$_3$/TiO$_2$ and V$_2$O$_5$/WO$_3$/TiO$_2$) supported metal oxide catalysts at 400°C. At low surface coverages (<0.2 monolayer) the dehydrated surface vanadium, chromium, rhenium, niobium, molybdenum and tungsten oxide species supported on titania generally tend to possess four-fold coordination and are predominately isolated. Whereas, at high surface coverages (>0.6 monolayer), the coordination of the dehydrated surface metal oxide species depends on the specific metal oxide and polymerized surface species are also usually present

(surface vanadia, chromia, molybdena, tungsta and niobia). Four-fold coordination is preferred for surface rhenium oxide, chromium oxide and vanadium oxide species, while six-fold coordination is preferred for surface iron oxide, molybdenum oxide, tungsten oxide and niobium oxide species. The observation that the turnover frequency for SO$_2$ oxidation over all of these catalysts is approximately the same at both low and high surface coverages indicates that the mechanism of sulfur dioxide oxidation is not sensitive to the coordination of the surface metal oxide species. Furthermore, SO$_2$ oxidation occurs at similar rates over both isolated and polymerized surface metal oxide species, which is expected for a reaction requiring only one active site.

The redox properties of the titania supported metal oxide catalysts have also been probed with the partial oxidation of methanol to formaldehyde and followed the trend V$_2$O$_5$–Re$_2$O$_7$>CrO$_3$–MoO$_3$>Nb$_2$O$_5$–WO$_3$ [78,128–130]. The yield of selective oxidation products (e.g., formaldehyde, methyl formate, dimethoxy methane) for supported niobium oxide and tungsten oxide catalysts were approximately two orders of magnitude less than for supported vanadium oxide and rhenium oxide. Tungsten oxide was shown to increase the yield of acid products (e.g., dimethyl ether). In addition, a very similar trend was observed for methanol oxidation over niobia supported metal oxide catalysts (V$_2$O$_5$>CrO$_3$>Re$_2$O$_7$>MoO$_3$>WO$_3$) [131]. These trends indicate that V$_2$O$_5$/TiO$_2$, Re$_2$O$_7$/TiO$_2$, CrO$_3$/TiO$_2$, MoO$_3$/TiO$_2$ and to a lesser degree Nb$_2$O$_5$/TiO$_2$ and WO$_3$/TiO$_2$ possess surface redox sites which can efficiently catalyze sulfur dioxide oxidation to sulfur trioxide.

The reactivity studies of the binary catalysts suggest that all of the surface species present in the ternary catalysts (i.e., oxides of V, Fe, Re, Cr, Nb, Mo and W) can undergo redox cycles and oxidize sulfur dioxide to sulfur trioxide to some extent. A comparison of the activities of the ternary catalysts with the corresponding binary catalysts indicates that the vanadium oxide and the additive supported metal oxide surface redox sites are acting independently without synergistic interactions, since the sum of the activities of the individual binary catalysts may be added to yield the activity of the corresponding ternary catalyst system. The absence of synergistic interactions is expected for single-site reactions such as sulfur

dioxide oxidation, whereas dual site reactions, e.g., SCR of NO_x, will exhibit an increase in turnover frequency as surface coverage increases.

The results found by Dunn et al. confirm the observation of Morikawa et al. [7] that V_2O_5/TiO_2 catalysts promoted by WO_3 or MoO_3 exhibit higher rates of sulfur dioxide oxidation than unpromoted catalysts. However, the TOFs for WO_3/TiO_2 and MoO_3/TiO_2 are significantly lower than the TOF for V_2O_5/TiO_2.

In contrast to the results of Dunn et al., Sazonova et al. [9] reported that the addition of high loadings of tungsten oxide to a V_2O_5/TiO_2 catalyst substantially suppresses sulfur dioxide oxidation activity. However, Sazonova et al. failed to recognize that for the loadings of surface vanadia ($\sim$3 monolayers) and tungsten oxide ($\sim$6 monolayers) species used in their study, the surface species are no longer molecularly dispersed and form WO_3 and V_2O_5 crystallites. Since no information about the structures or dispersions of the metal oxides was presented, it is not possible to clearly identify the reason for the decrease in oxidation activity, but is most likely due to the presence of the metal oxide crystalline phases, which are not very active for redox reaction [37,38,128].

It has been proposed that electronic interactions between neighboring surface vanadia and tungsten oxide sites on a titania support may lead to an increase in sulfur dioxide oxidation activities at temperatures below 230°C [131]. However, more recent studies probing the redox properties of ternary $V_2O_5/WO_3/TiO_2$ catalysts at 200°C and 230°C by the single-site sulfur dioxide oxidation and selective oxidation of methanol to formaldehyde reactions failed to detect an increase in redox activity for the ternary catalyst with respect to the corresponding binary catalysts [17]. Therefore, there does not appear to be any evidence that electronic interactions between surface vanadia and surface tungsten oxide species of ternary catalysts allow redox reactions to proceed more efficiently.

5.1.5. Influence of the sulfate overlayer

The surface sulfate species present on sub-monolayer supported vanadia catalysts preferentially coordinate with the oxide supports rather than the surface vanadia species under dehydrated conditions and, consequently, can only indirectly affect the molecular structures of the supported vanadia species via lateral interactions [93]. Surface sulfate species can also undergo redox cycles and promote the oxidation of SO_2 to SO_3 at elevated temperatures. However, for reaction temperatures below 400°C, the surface sulfates can be regarded as spectator species since they do not undergo redox cycles at any appreciable rate. In addition, surface sulfates may volatilize upon increasing temperature before any tangible enhancement in oxidation activity is observed [98].

The formation of sulfate overlayers on sub-monolayer supported vanadia catalysts requires that special care be taken in measuring sulfur dioxide oxidation kinetics over these catalysts. The measured rate of SO_2 oxidation over fresh (non-sulfated) catalysts may be either over or underestimated, depending on the experimental methodology, for the first several hours of reaction time due to the in situ development of the surface sulfate overlayer [121].

5.2. Kinetics of SO_2 oxidation

5.2.1. Effect of low SO_2 adsorption probability on reaction rate

The reason for the extremely low sulfur dioxide oxidation turnover frequencies exhibited by monolayer supported vanadia catalysts (3.7×10^{-6} s^{-1} for V_2O_5/SiO_2–2.2×10^{-4} s^{-1} for V_2O_5/CeO_2 at 400°C [17]) may be either that:

1. the quantity of vanadium oxide–sulfur oxide surface complexes formed under reaction conditions is very low, however, once formed the surface complexes readily decompose to produce sulfur trioxide (low adsorption probability and fast rate determining step),
2. large numbers of stable surface complexes are formed, which is slowly react to produce sulfur trioxide (high adsorption probability and slow rate determining step), or
3. small numbers of stable surface complexes are formed (low adsorption probability and slow rate determining step).

As long as the surface coverage of adsorbed SO_2 species is not so high as to be limited by steric factors, the number of vanadium oxide–sulfur oxide surface complexes formed at a certain temperature, as determined by adsorption experiments, can be viewed as

the maximum number of surface vanadia sites capable of simultaneously undergoing redox cycles at that temperature. The observation that the adsorption and oxidative adsorption of SO_2 onto monolayer supported vanadia catalysts at temperatures between 80°C and 150°C is negligible rules out option (2) [67–69,103]. Thus, consistent with options (1) and (3) above, it appears that the low SO_2 oxidation turnover frequencies of monolayer supported vanadia catalysts may be due to a lack of surface vanadia sites adsorbing sulfur dioxide and undergoing redox cycles under reaction conditions (low adsorption probability). Since no data regarding the fundamental rate of vanadium oxide–sulfur oxide surface complex decomposition to products are currently found in the literature, it is not possible to distinguish between the options of fast or slow rate determining step.

5.2.2. Effect of reaction environment

Qualitative data detailing the effects of complicated reaction environments on SO_2 oxidation kinetics over industrial-type catalysts can be found in the literature [18]. Unfortunately, limited information is presented in these studies as to the effects of the various reaction gases on the structure of the surface vanadia species. Therefore, in an effort to relate reaction kinetics with well characterized catalytic systems, the effects of only oxygen, water vapor and sulfur oxide partial pressures on SO_2 oxidation kinetics will be addressed in detail since the effects of these gases on the molecular structures of supported vanadia catalysts are well understood.

5.2.2.1. Effect of oxygen. Several studies using a reaction gas mixture containing approximately 1000 ppm of SO_2 have confirmed that when oxygen partial pressures are varied above 1 vol%, the rate of SO_2 oxidation over dehydrated vanadia catalysts is nearly constant (i.e., the reaction rate is independent (zero-order) of the gas phase oxygen partial pressure) [8,17,18]. When the oxygen partial pressure is varied between 0.1 and 1 vol% oxygen, the dependence of the rate of oxidation on the gas phase oxygen partial pressure was seen to be approximately half-order [17]. Thus, in the case of industrial conditions traditionally experienced by supported vanadia catalysts (e.g., 2–6 vol% oxygen), the catalyst surface is essentially saturated with adsorbed

oxygen and the surface vanadia species are essentially present in the V^{5+} state possessing dehydrated isolated and polymerized VO_4 structures (see Section 4.1 above).

5.2.2.2. Effect of sulfur oxides. The influence of sulfur dioxide partial pressure on the rate of oxidation requires a more complex analysis due to the presence of the product sulfur trioxide, which may compete with sulfur dioxide for adsorption on the surface vanadia species. The basicity of the bridging oxygen in the V–O–M bond appears to be responsible for influencing the adsorption of acidic molecules on the surface vanadia species. The electronic structures of sulfur dioxide and sulfur trioxide molecules in the gas phase indicate the electron deficiency of the sulfur atom and, consequently, the acidity of the sulfur in the resonance hybrid structure for sulfur trioxide (+2) is higher than that for sulfur dioxide (+1). As a result, sulfur trioxide will experience a greater attraction to the electrons of the bridging oxygen of the V–O–M bond, resulting in a preferential adsorption of sulfur trioxide. This results in a stronger bonding of sulfur trioxide to the surface vanadia species and, consequently, competitive adsorption with sulfur dioxide [17].

When product inhibition by sulfur trioxide is not taken into account, the apparent reaction rate dependence on gas phase sulfur dioxide concentration for vanadia supported catalysts can be crudely fitted to a half-order dependence. However, assuming competitive adsorption of sulfur trioxide the rate dependence on sulfur dioxide concentration was shown to be first-order with a negative first-order dependence on sulfur trioxide. Thus, the SO_2 oxidation reaction over supported vanadia catalysts exhibits a first-order dependence on SO_2 partial pressures and a negative first-order dependence on SO_3 partial pressures [17].

5.2.2.3. Effect of water vapor. The addition of water to the reaction mixture of SO_2, O_2 and SO_3 results in a significant decrease in SO_2 conversion over supported vanadia catalysts [18]. For temperatures above 300°C, the inhibiting effect of water results in an approximate 50% decrease in reaction rate. The rate of reaction was shown to be practically independent of the concentration of water vapor in the range of

practical interest in many air pollution control applications (e.g., 5–15 vol%). If the flow of water is stopped the original activity measured in the absence of water vapor is restored within approximately 1 h and then remains constant. The inhibition by water is likely explained in terms of reversible site blockage of the surface vanadia active sites for sulfur dioxide adsorption/oxidation. At reaction temperatures between 200°C and 300°C sub-monolayer quantities of adsorbed water form on the catalytic surface and are expected to drastically decrease the oxidation rate [82]. The oxidation activity will not be restored until the moisture is desorbed at temperatures above 300°C.

5.2.2.4. Effect of other gases (NO$_x$ and NH$_3$). A comprehensive study on the effects of gases typically found in SCR DeNO$_x$ applications on the SO$_2$ oxidation activity of an industrial V$_2$O$_5$/WO$_3$/TiO$_2$ catalyst was conducted by Forzatti and co-workers [18]. The addition of low concentrations of ammonia (~100 ppm NH$_3$) to a reaction stream containing 1000 ppm of SO$_2$ and 2% O$_2$ was found to strongly inhibit SO$_2$ oxidation at 330°C and resulted in a 90% reduction in SO$_2$ oxidation activity. When the flow of ammonia was stopped the SO$_2$ oxidation activity returned to about 90% of its original value within 3 h. The inhibition by ammonia is likely to explained in terms of reversible site blockage of the surface vanadia sites responsible for sulfur dioxide adsorption/oxidation. Nitric oxide was shown to have a much smaller effect and neither significantly increased nor decreased the catalyst's SO$_2$ oxidation activity. This indicates that under the prescribed experimental conditions nitric oxide, unlike water and ammonia, does not block the active vanadia sites. The simultaneous addition of NH$_3$ and NO to the reaction stream yielded a net-inhibiting effect for NH$_3$:NO ratios greater than 0.4.

5.2.2.5. Effect of reaction temperature. The temperature dependence of the oxidation of SO$_2$ to SO$_3$ over a series of supported vanadia catalysts was investigated using a reactant mixture of 1000 ppm SO$_2$, 18% O$_2$ and balance He. In view of the results previously discussed, the data were analyzed by assuming a differential plug-flow reactor model and a rate equation first-order in SO$_2$, zero-order in O$_2$ and

negative first-order in SO$_3$:

$$r_{SO_2} = \frac{k[SO_2][O_2]^0}{[SO_3]} \qquad (1)$$

The apparent activation energy of 21±2 Kcal/mol was approximately constant as surface vanadia coverage on a titania supported catalysts was varied between 0.16 and 1.0 theoretical monolayers (1.5–8 V atoms/nm^2) [17]. Essentially the same activation energy was found for SO$_2$ oxidation over ceria, zirconia, alumina and silica supported vanadia catalysts.

5.3. Mechanism of SO$_2$ oxidation

Numerous mechanisms for the oxidation of SO$_2$ over supported V$_2$O$_5$/TiO$_2$ catalysts have been proposed [8,17,18]. Forzatti and coworkers [18] proposed that the active site for the oxidation of sulfur dioxide over V$_2$O$_5$/TiO$_2$ catalysts involved a dimeric vanadia sulfate species, which is in disagreement with the findings of Wachs and coworkers [17] that SO$_2$ oxidation requires only a single vanadia surface site. The inability of the currently available spectroscopic techniques to elucidate the molecular structure of the vanadium oxide–sulfur oxide surface complexes, which must be formed under reaction conditions, prevents the validation of any one of these mechanisms. Furthermore, the failure of thermal techniques (e.g., TGA and TPD) to provide information regarding the rates of adsorption and desorption of SO$_2$ and SO$_3$ on the active vanadia sites prevents a clear determination of the rate determining step of the SO$_2$ oxidation reaction over these catalysts. It has been proposed that in situ spectroscopic studies of the SO$_2$ oxidation reaction over monolayer supported vanadia catalysts using isotope-exchanged reactants (e.g., ^{18}O$_2$, S^{18}O$_2$, S^{18}O$_3$, etc.) may be able to clarify some of the issues that must be addressed before a sound proposal for a mechanism can be made [121].

However, based on the currently available kinetic information it is possible to theorize a general reaction pathway for SO$_2$ oxidation over supported vanadia catalysts [17]. Sulfur dioxide may adsorb and coordinate onto the vanadium–oxygen–support (V–O–M) bond of either isolated or polymerized surface (M–O)$_3$V^{+5}=O sites resulting in either the (V^{+5})·SO$_2$-ads or the (V^{+3})·SO$_3$-ads state. This is followed by the

cleavage of the V^{+5}–O–SO_2 or M–O–SO_2 bond and formation of $SO_{3(g)}$, which represents the rate determining step. The electron deficiency and, consequently, the acidity of the sulfur in the resonance hybrid structure for SO_3 (i.e., +2) is higher than that for SO_2 (i.e., +1). As a result, sulfur trioxide will experience a greater attraction to the electrons of the bridging oxygen of the V–O–M bond, resulting in a preferential adsorption of SO_3. This results in a stronger bonding of SO_3 to the surface vanadia species and, consequently, competitive adsorption on (V^{+5}) sites. The reduced vanadia site is then reoxidized by dissociatively adsorbed oxygen, thereby regenerating the active (V^{+5}) sites.

6. Conclusions

Comparison of the surface vanadia molecular structural information with the corresponding SO_2 oxidation reactivity data has provided some insights into the reactivity properties of the surface vanadia species for SO_2 oxidation to SO_3. At low vanadia loadings, surface vanadia preferentially exists on aluminum, titanium, zirconium and cerium oxide support surfaces as isolated $(M–O)_3V^{+5}$=O species. At higher vanadia loadings, the isolated $(M–O)_3V^{+5}$=O species also polymerize on the oxide support surface breaking V–O–M bonds and forming V–O–V bridging bonds. The bridging V–O–V and terminal V=O bonds do not appear to critically influence the reactivity properties of the surface vanadia species during SO_2 oxidation. The bridging V–O–support bond, however, appears to be the most critical bond since its properties can change the SO_2 oxidation turnover frequency by more than an order of magnitude. The basicity of the bridging V–O–M oxygen appears to be responsible for influencing the adsorption and subsequent oxidation of the acidic SO_2 molecule.

The turnover frequency for SO_2 oxidation is very low, 10^{-4}–10^{-5} s^{-1} at 400°C, due to the inability of the acidic surface vanadia species to efficiently adsorb SO_2 under reaction conditions and the inhibition of product SO_3. The observation that the SO_2 oxidation turnover frequency does not increase with increasing surface coverage by vanadia species suggests that only one surface vanadia site is necessary for the SO_2 oxidation to proceed.

A systematic catalytic investigation of the SO_2 oxidation reactivity of several binary (M_xO_y/TiO_2) and ternary $(V_2O_5/M_xO_y/TiO_2)$ supported metal oxide catalysts revealed that the SO_2 oxidation turnover frequencies of the binary catalysts were all within an order of magnitude $(V_2O_5/TiO_2 > Fe_2O_3/TiO_2 > Re_2O_7/TiO_2 – CrO_3/TiO_2 – Nb_2O5/TiO_2 > MoO_3/TiO_2 – WO_3/TiO_2)$. The observation that the turnover frequency for SO_2 oxidation over all of these catalysts is approximately the same at both low and high surface coverages indicates that the mechanism of sulfur dioxide oxidation is not sensitive to the coordination of the surface metal oxide species. Furthermore, SO_2 oxidation occurs at similar rates over both isolated and polymerized surface metal oxide species, which is expected for a reaction requiring only one active surface site.

A comparison of the activities of the ternary catalysts with the corresponding binary catalysts suggests that the surface vanadium oxide and the additive surface oxide redox sites act independently without synergistic interactions, since the sum of the individual activities of the binary catalysts quantitatively correspond to the activity of the corresponding ternary catalyst. These observations are consistent with structural characterization studies, which showed very limited interactions among the surface metal oxide species and the one site requirement of the SO_2 oxidation reaction.

The rate of sulfur dioxide oxidation over supported vanadia catalysts is zero-order in oxygen, first-order in sulfur dioxide and inhibited by sulfur trioxide under typical industrial conditions. The apparent activation energy for sulfur dioxide oxidation over these supported vanadia catalysts was approximately 21 Kcal/mol. The SO_2 oxidation reaction is also inhibited by gaseous molecules that readily adsorb on the surface vanadia sites (e.g., H_2O, NH_3, etc.).

References

[1] C.D. Cooper, F.C. Alley, Air Pollution Control: A Design Approach, Waveland Press, Prospect Heights, IL, 1994.

[2] Chem. Eng. News, 23 June (1997) 42.

[3] A. Urbanek, M. Trela, Catal. Rev.-Sci. Eng. 21(1) (1980) 73.

[4] B. Balzhinimaev, A. Ivanov, O. Lapina, V. Mastikhin, K. Zamaraev, Faraday Discuss. Chem. Soc. 87 (1989) 133.

[5] O. Lapina, V. Mastikhin, A. Shubin, V. Krasilnikov, K. Zamaraev, Prog. NMR Spectrosc. 24 (1992) 457.

[6] H. Bosch, F.J.J.G. Janssen, Catal. Today 2 (1988) 369.

[7] S. Morikawa, H. Yoshida, K. Takahashi, S. Kurita, Chem. Lett. (1981) 251.

[8] S. Morikawa, H. Yoshida, K. Takahashi, S. Kurita, Proceedings of the Eighth International Congress on Catalysis, 1984, p. 661.

[9] N. Sazonova, L. Tsykoza, A. Simakov, G. Barannik, Z. Ismagilov, React. Kinet. Catal. Lett. 52(1) (1994) 101.

[10] M. Imanari, Y. Watanbe, Proceedings of the Eighth International Congress on Catalysis, 1984, p. 841.

[11] B.S. Shin, S.Y. Lim, S.J. Choung, Korean J. Chem. Eng. 11(4) (1994) 254.

[12] J. Armor, Appl. Catal. B 1 (1992) 221.

[13] N. Ohlms, Catal. Today 16(2) (1993) 247.

[14] A.A. Bhattacharyya, G.M. Woltermann, J.S. Yoo, J.A. Karch, W.E. Cormier, Ind. Eng. Chem. Res. 27 (1988) 1356.

[15] A. Corma, A.E. Palomares, F. Rey, Appl. Catal. B 4 (1994) 29.

[16] J.S. Buchanan, D.L. Stern, K.E. Nariman, G.J. Teitman, J.F. Sodomin, D.L. Johnson, Ind. Eng. Chem. Res. 35(8) (1992) 2495.

[17] J.P. Dunn, P.R. Koppula, H.G. Stenger, I.E. Wachs, Appl. Catal. B: Env. 19 (1998) 103.

[18] J. Svachula, L. Alemany, N. Ferlazzo, P. Forzatti, E. Tronconi, F. Bregani, Ind. Eng. Chem. Res. 32 (1993) 826.

[19] J. Haber, A. Kozlowska, R. Kozlowsi, J. Catal. 102 (1986) 52.

[20] M.M. Koranne, J.G. Goodwin, G. Marcelin, J. Catal. 148 (1994) 369.

[21] G.C. Bond, K. Bruckman, Faraday Disc. Chem. Soc. 72 (1981) 235.

[22] G. Deo, I.E. Wachs, J. Catal. 146 (1994) 323.

[23] G. Deo, I.E. Wachs, J. Catal. 146 (1994) 335.

[24] A.J. van Hengstrum, J.G. van Ommen, H. Bosch, P.J. Gellings, Appl. Catal. 8 (1983) 369.

[25] I.E. Wachs, R.Y. Saleh, S.S. Chan, C.C. Chersich, Appl. Catal. 15 (1985) 339.

[26] H. Knozinger, E. Taglauer, Catalysis 10 (1993) 1.

[27] G. Hausinger, H. Schmelz, H. Knozinger, Appl. Catal. 39 (1988) 267.

[28] J. Haber, T. Machej, E.M. Serwicka, I.E. Wachs, Catal. Lett. 32 (1995) 101.

[29] J. Haber, T. Machej, T. Czeppe, Surf. Sci. 151 (1985) 301.

[30] T. Machej, J. Haber, A.M. Turek, I.E. Wachs, Appl. Catal. 70 (1991) 115.

[31] G. Centi, D. Pinelli, Trifiro, in: R. Gasselli, A. Sleight (Eds.), Structure-Activity Relationships in Heterogeneous Catalysis, Elsevier, Amsterdam, 1990, p. 1.

[32] N. Das, H. Eckert, H. Hu, I.E. Wachs, J.F. Walzer, F.J. Feher, J. Phys. Chem. 97 (1993) 8240.

[33] G.T. Went, S.T. Oyama, J. Phys. Chem. 94 (1990) 4240.

[34] H. Eckert, I.E. Wachs, Mater. Res. Soc. Symp. Proc. 111 (1988) 455.

[35] H. Eckert, I.E. Wachs, J. Phys. Chem. 93 (1989) 6796.

[36] U. Scharf, M. Schraml-Marth, A. Wokaun, A. Baiker, J. Chem. Soc., Faraday Trans. 87 (1991) 3299.

[37] G. Deo, I.E. Wachs, J. Haber, Crit. Rev. Surf. Chem. 4(3)(4) (1994) 141.

[38] I.E. Wachs, B.M. Weckhuysen, Appl. Catal. A 157 (1997) 67.

[39] M.A. Vuurman, A.M. Hirt, I.E. Wachs, J. Phys. Chem. 95 (1991) 9928.

[40] I.E. Wachs, J.M. Jehng, G. Deo, B.M. Weckhuysen, V.V. Guliants, J. Benziger, Catal. Today 32 (1996) 47.

[41] F.D. Hardcastle, I.E. Wachs, Catal. R. Soc. Chem. 10 (1993) 102.

[42] I.E. Wachs, Catal. Today 27 (1996) 437.

[43] G. Busca, Mater. Chem. Phys. 19 (1988) 157.

[44] A.A. Davydov, Kinet. Katal. 34 (1993) 951.

[45] A.M. Turek, I.E. Wachs, E. De Canio, J. Phys. Chem. 96 (1992) 5000.

[46] H. Knozinger, in: D.D. Eley, H. Pines, P.B. Weisz, (Eds.), Advances in Catalysis, vol. 25, Academic Press, New York, 1976.

[47] C.R. Brundle, C.A. Evans, Jr., S. Wilson (Eds.), Encyclopedia of Materials Characterization, Butterworth-Heinemann, Stoneham, 1992.

[48] L.R. Le Costumer, B. Taouk, M. Le Meur, E. Payen, M. Guelton, J. Grimblot, J. Phys. Chem. 92 (1988) 1230.

[49] T. Tanaka, H. Yamashita, R. Tsuchitania, T. Funabiki, S. Yoshida, J. Chem. Soc., Faraday Trans. 84(1) (1988) 2897.

[50] S. Yoshida, T. Tanaka, Y. Nishimura, H. Mizutani, in: J. Phillips, M. Ternan (Eds.), Proceedings of the Ninth International Congress on Catalysis, vol. 3, 1988, p. 1473.

[51] S. Yoshida, T. Tanaka, T. Hanada, T. Hiraiwa, H. Kanai, Catal. Lett. 12 (1992) 277.

[52] G. Busca, E. Giamello, Mater. Chem. Phys. 25(5) (1990) 475.

[53] P. Brant, R.Y. Saleh, I.E. Wachs, unpublished results.

[54] S. Yoshida, T. Iguchi, S. Ichida, K. Tarama, Bull. Chem. Soc. Jpn. 45 (1972) 376.

[55] M. Inomata, K. Mori, A. Miyato, Y. Murakami, J. Phys. Chem. 87 (1983) 761.

[56] K.V.R. Chary, R.B. Mahipal, N.K. Nag, V.S. Subrahmanyam, C.S. Sumanda, J. Phys. Chem. 88 (1984) 2622.

[57] P. Fejes, I. Marsi, I. Kirisci, J. Halasz, J. Hannus, A. Rockenbaur, G. Tasi, L. Korecz, G. Schobel, Stud. Surf. Sci. Catal. 69 (1991) 173.

[58] P. Ciambelli, L. Lisi, G. Russo, J.C. Volta, Appl. Catal. B 7 (1995) 1.

[59] M.C. Paganini, L. Dall'Acqua, E. Giamello, L. Lietti, P. Forzatti, G. Busca, J. Catal. 166 (1997) 195.

[60] B.M. Weckhuysen, R.A. Schoonheydt, G. Deo, H. Hu, J.M. Jehng, I.E. Wachs, Paper presented at 13th North American Catalysis Society Meeting, Salt Lake City, Utah, June 1995.

[61] B.M. Weckhuysen, I.P. Vannijvel, R.A. Schoonheydt, Zeolites 15 (1995) 482.

[62] U. Scharf, M. Schraml-Marth, A. Wokaun, A. Baiker, J. Chem. Soc., Faraday Trans. 87 (1991) 3299.

[63] M. Fournier, C. Louis, M. Che, P. Chauquin, D. Masure, J. Catal. 119 (1990) 400.

[64] B.A. Morrow, J.L.G. Fierro (Eds.), Spectroscopic Characterization of Heterogeneous Catalysts, Part A. Methods of Surface Analysis, Elsevier, Amsterdam, 1990.

[65] J. Datka, A.M. Turek, J.M. Jehng, I.E. Wachs, J. Catal. 135 (1992) 186.

[66] H. Miyata, K. Fuji, T. Ono, J. Chem. Soc., Faraday Trans. 81(1) (1988) 3121.

[67] J. Le Bars, A. Auroux, J. Therm. Anal. 40 (1993) 1277.

[68] J. Le Bars, J.C. Vedrine, A. Auroux, S. Trautmann, M. Baerns, Appl. Catal. A 119 (1994) 341.

[69] J. Le Bars, A. Auroux, M. Frorissier, J.C. Vedrine, J. Catal. 162 (1996) 250.

[70] X. Gao, I.E. Wachs, in preparation.

[71] G.T. Went, S.T. Oyama, J. Phys. Chem. 94 (1990) 4240.

[72] J. Hanuza, B. Jezowska-Trzebiatowska, W. Oganowski, J. Mol. Catal. 29 (1985) 109.

[73] H. Eckert, G. Deo, I.E. Wachs, in preparation.

[74] G. Deo, Ph.D. Dissertation, Lehigh University, USA, 1992.

[75] M.A. Vuurman, I.E. Wachs, J. Mol. Catal. 77 (1992) 29.

[76] M.A. Vuurman, D.J. Stufkens, A. Oskam, G. Deo, I.E. Wachs, J. Chem. Soc., Faraday Trans. 92 (1996) 3259.

[77] A. Andreini, M. De Boer, M.A. Vuurman, G. Deo, I.E. Wachs, J. Chem. Soc., Fararday Trans. 92 (1996) 3267.

[78] G. Deo, I.E. Wachs, J. Catal. 146 (1994) 335.

[79] G. Ramis, G. Busca, F. Bregani, Catal. Lett. 18 (1993) 299.

[80] W. Harding, K.E. Birkeland, H.H. Kung, Catal. Lett. 28 (1994) 1.

[81] L. Owens, H.H. Kung, J. Catal. 148 (1994) 587.

[82] J.M. Jehng, G. Deo, B.M. Weckhuysen, I.E. Wachs, J. Mol. Catal. A 110 (1996) 41.

[83] M. Waqif, A.M. Saad, M. Bensitel, J. Bacheller, O. Saur, J.C. Lavalley, J. Chem. Soc., Faraday Trans. 88(19) (1992) 2931.

[84] B.A. Morrow, R.A. McFarlane, M. Lion, J.C. Lavalley, J. Catal. 107 (1987) 232.

[85] O. Saur, M. Bensitel, A.B. Mohammed Saad, J.C. Lavalley, C.P. Tripp, B.A. Morrow, J. Catal. 99 (1986) 104.

[86] M. Bensitel, O. Saur, J.C. Lavalley, B.A. Morrow, Mater. Chem. Phys. 19 (1988) 147.

[87] W. Waqif, P. Bazin, O. Saur, J.C. Lavalley, G. Blanchard, O. Touret, Appl. Catal. B 11 (1997) 193.

[88] M. Ziolek, J. Kujawa, O. Saur, A. Aboulayt, J.C. Lavalley, J. Mol. Catal. 112 (1996) 125.

[89] A. Pieplu, O. Saur, J.C. Lavalley, M. Pijolat, O. Legendre, J. Catal. 159 (1996) 394.

[90] J. Twu, C.J. Chuang, K.I. Chang, C.H. Yang, K.H. Chen, Appl. Catal. B 12(4) (1997) 309.

[91] A.B.M. Saad, O. Saur, Y. Wang, C.P. Tripp, B.A. Morrow, J.C. Lavalley, J. Phys. Chem. 99(13) (1995) 4620.

[92] Y. Okamoto, T. Imanaka, J. Phys. Chem. 92 (1988) 7102.

[93] J.P. Dunn, J.M. Jehng, D.S. Kim, L.E. Briand, H.G. Stenger, I.E. Wachs, J. Phys. Chem. 102 (1998) 6212.

[94] T. Yamaguchi, K. Tanabe, J. Phys. Chem 90 (1986) 3148.

[95] T. Yamaguchi, T. Jin, T. Ishida, K. Tanabe, Mater. Chem. Phys. 17 (1987) 3.

[96] K.E. Smith, V.E. Henrich, J. Vac. Sci. Technol. A 7(3) (1989) 1967.

[97] I.G. Dalla Lana, H.G. Karge, Z.M. George, J. Phys. Chem. 97 (1993) 8005.

[98] M. Waqif, O. Saur, J.C. Lavalley, Y. Wang, B.A. Morrow, Appl. Catal. 71 (1991) 319.

[99] J.S. Yoo, A.A. Bhattacharyya, C.A. Radlowski, J.A. Karch, Appl. Catal. B 1 (1992) 169.

[100] A. Bhattacharyya, J.S. Yoo, in: J.S. Magee, M.M. Mitchell, Jr. (Eds.), Fluid Catalytic Cracking: Science and Technology, Stud. Surf. Sci. Catal. vol. 76, (1993).

[101] A. Corma, A.E. Palomares, F. Rey, Appl. Catal. B 4 (1994) 29.

[102] T. Yamaguchi, Appl. Catal. 61 (1990) 1.

[103] W.S. Kijlstra, N.J. Komen, A. Andreini, E.K. Poels, A. Bliek, Proceedings of the 11th International Congress on Catalysis, Stud. Surf. Sci. Catal. 101 (1996) 951.

[104] G. Busca, H. Saussey, O. Saur, J.C. Lavalley, V. Lorenzelli, Appl. Catal. 14 (1985) 245.

[105] M. Waqif, J. Bachelier, O. Saur, J.C. Lavalley, J. Mol. Catal. 72 (1992) 127.

[106] G. Busca, G. Ramis, R.J. Willey, E. Astorino, F. Bregani, G. Centi (Eds.), Environmental Catalysis, SCI Publishers, Rome, Italy, 1995.

[107] J. Preud'Homme, J. Lamotte, A. Janin, J.C. Lavalley, Bull. Soc. Chim. France 1(11)(12) (1981) 433.

[108] M. Bensitel, M. Waqif, O. Saur, J.C. Lavalley, J. Phys. Chem. 93 (1989) 6581.

[109] J.P. Chen, R.T. Yang, J. Catal. 125 (1990) 411.

[110] J.P. Chen, R.T. Yang, J. Catal. 139 (1993) 277.

[111] M.D. Amaridis, I.E. Wachs, G. Deo, J.M. Jehng, D.S. Kim, J. Catal. 161 (1996) 247.

[112] P. Ciambelli, M.E. Fortuna, D. Sannino, A. Baldacci, Catal. Today 29 (1996) 161.

[113] J. Haber, A. Kozlowska, R. Kozlowski, J. Catal. 102 (1986) 52.

[114] M.M. Koranne, J.G. Goodwin Jr., G. Marcelin, J. Catal. 148 (1994) 369.

[115] N.K. Nag, F.E. Massoth, J. Catal. 124 (1990) 127.

[116] M.A. Eberhardt, A. Proctor, M. Houalla, D.M. Hercules, J. Catal. 160 (1996) 27.

[117] M.L. Rojascervantes, A.J. Lopezpeinado, J.D. Lopesganzales, Carrascomarin, J. Mater. Sci. 31 (1996) 437.

[118] B. Jonson, B. Rebenstorf, R. Larrson, S.L.T. Andersson, J. Chem. Soc., Faraday Trans. 84(1) (1988) 1897.

[119] M.A. Banares, X. Gao, I.E. Wachs, in preparation.

[120] S. Contakes, I.E. Wachs, in preparation.

[121] J.P. Dunn, Ph.D. Dissertation, Lehigh University, USA, 1998.

[122] A. Yasmin, J. Ross, J.M. Jehng, I.E. Wachs, unpublished results.

[123] I.E. Wachs, J.M. Jehng, G. Deo, B.M. Weckhuysen, V.V. Guliants, J.B. Benziger, S. Sundaresan, J. Catal. 170(1) (1997) 75.

[124] G. Deo, I.E. Wachs, J. Catal. 146(2) (1994) 323.

[125] R.T. Sanderson, J. Chem. Ed. 65(2) (1988) 112.

[126] I.E. Wachs, Catalysis, vol. 13, Royal Society of Chemistry, Cambridge, 1997.

[127] J.P. Dunn, H.G. Stenger, I.E. Wachs, J. Catal. 181 (1999) 233.

[128] I.E. Wachs, G. Deo, D.S. Kim, M.A. Vuurman, H. Hu, J. Mol. Catal. 83 (1993) 443.

[129] D. Deo, J.M. Jehng, D.S. Kim, I.E. Wachs, M.A. Vuurman, A. Andreini, in: G. Centi et al. (Eds.), Environmental Catalysis, SCI Publishers, Rome, 1995, p. 207 .

[130] J.M. Jehng, I.E. Wachs, Catal. Today 8 (1990) 37.

[131] L. Lietti, P. Forzatti, F. Bregani, Ind. Eng. Chem. Res. 35 (1996) 3884.